Scientific Research Publishing

Journal of Applied Mathematics and Physics, 2022, 10, 1785-1812
https://www.scirp.org/journal/jamp
ISSN Online: 2327-4379
ISSN Print: 2327-4352

Golden Quartic Polynomial and Moebius-Ball Electron

Hans Hermann Otto

Materials Science and Crystallography, Clausthal University of Technology, Clausthal-Zellerfeld, Germany
Email: hhermann.otto@web.de

How to cite this paper: Otto, H.H. (2022) Golden Quartic Polynomial and Moebius-Ball Electron. *Journal of Applied Mathematics and Physics*, **10**, 1785-1812.
https://doi.org/10.4236/jamp.2022.105124

Received: April 7, 2022
Accepted: May 28, 2022
Published: May 31, 2022

Abstract

A symmetrical quartic polynomial, named golden one, can be connected to coefficients of the icosahedron equation as well as to the gyromagnetic correction of the electron and to number 137. This number is not a mystic one, but is connected with the inverse of *Sommerfeld*'s fine-structure constant and this way again connected with the electron. From number-theoretical realities, including the reciprocity relation of the golden ratio as effective precalculator of nature's creativeness, a proposed closeness to the icosahedron may point towards the structure of the electron, thought off as a single-strand compacted helically self-confined charged elemantary particle of less spherical but assumed blunted icosahedral shape generated from a high energy double-helix photon. We constructed a chiral *Moebius* "ball" from a 13 times 180˚ twisted double helix strand, where the turning points of 12 generated slings were arranged towards the vertices of a regular icosahedron, belonging to the non-centrosymmetric rotation group *I532*. Mathematically put, we convert the helical motion of an energy quantum into a stationary motion on a *Moebius* stripe structure. The radius of the ball is about the *Compton* radius. This chiral closed circuit *Moebius* ball motion profile can be tentatively thought off as the dominant quantum vortex structure of the electron, and the model may be named *CEWMB* (**C**harged **E**lectromagnetic **W**ave **M**oebius **B**all). Also the gyromagnetic factor of the electron (g_e = 2.002319) can be traced back to this special structure. However, nature's energy infinity principle would suggest a superposition with additional less dominant (secondary) structures, governed also by the golden mean. A suggestion about the possible structure of delocalized hole carriers in the superconducting state is given.

Keywords

Golden Qartic Polynomial, Number Theory, Icosahedron Equation, Golden Mean, Fifth Power of the Golden Mean, *Moebius* Ball, Electron Structure, Chirality, Fine-Structure Constant, *Fibonacci* Number 13, *Lucas* Numbers,

Superconductivity

1. Introduction

In this contribution, we dealt with the question, what indeed could be the relationship between a helical photon and a compacted elementary entity like the electron, composed of a burst helical photon, and why is an electron as stable as it is? We here apply dominant principles of nature such as symmetry, golden ratio sophistication, reciprocity, calculus, eternal repetition and entanglement. In this way, helical twisting is a frequently observed tool in nature's quiver, applied to objects from microscopic to cosmic scale. When we were children, we played with twisted twine that, after being folded at half the length, became stable double helically curled cords of chosen chirality. As a crystallographer, I explained chirality using a coil spring that, when rotated about 180˚, maintained the sense of curling, but when looked in front of a mirror, the image showed an opposite sense of chirality. This may help to understand the new exciting theories about the structure of the photon and the electron as helically curled wavy entities or self-confined elementary particles derived from compacted photons, quoting only the most impressive references among many others [1] [2] [3] [4] [5].

Another extended publication by *Markoulakis and Antonidakis* [6], published at the beginning of this year, is highly recommended. What indeed happens, if a high-energy photon of sufficient energy hits matter, forming a pair of particles with opposed chirality (pair creation of the electron besides the positron)? Either the energy-rich helically twisted photon already consists of strands of opposite chirality respectively charge or different chirality is immediately generated when it hits matter to form the positron besides the electron. These fundamental particles may be formed from single strand "circular ribbons" of the photon maintaining twisting that were glued together like an odd multiply screwed *Moebius* strip. The relationship between geometry and physical properties of a simple *Moebius* strip can be followed by a contribution of *Starostin* and *Van der Heijden* [7]. However, the proposed *Moebius* ball is very more complicated to be tackled mathematically, but may nevertheless represent an energetically most favorable state.

Noticeably, helical left-handedness and its opposite could be realized, when a single cellulosic fiber helix or cucumber tendrils were supported at both ends to minimize the twisting energy [8] [9].

However, what can we say about an elliptically twisted helix structure of the photon in contrast to the postulated circular helical structure?

In all such considerations, the golden ratio should be involved as nature's effective-evolutionary pre-calculator, dominating all areas of science, life and cosmos. So we begin in Chapter 2 with a short essay of number theory and the

reciprocity property of this fundamental number. Doing this, we refer once again the extensive work done by *Olsen* on this subject [10] and recommend the contribution of *H. Weiss* and *V. Weiss* [11]. In Chapter 3, we deal with the golden ratio geometry of dual platonic solids proposed as envelope of electrons quantum vortex structure. Then, we explain in Chapter 4 the symmetrical double-well structure of the golden quartic polynomial as fundamental tool to understand nature's secrets, connecting number theory with the possible structure of elementary particles. *Sommerfeld*'s fine-structure constant as well as the gyromagnetic correction factor of the electron can be tackled with such an approach. This was done in the Chapters 5 and 6. We can construct a *Moebius* "ball" from a 13 times 180˚ twisted double helix strand, followed by a cut into two single strands, where the turning points of its 12 generated slings were arranged towards the vertices of a regular icosahedron. This closed circuit *Moebius* ball motion profile can be tentatively thought off as the dominant quantum vortex structure of the electron. This is the essential innovative aspect of the paper explained in Chapter 7. In Chapter 8 we try to tackle the secret of the structure of delocalized hole carrier strands in the superconducting state. Finally, in Chapter 9, the challenge for modeling of new inorganic respectively organic *Moebius* ball structures is outlined.

When dealing with non-orientable surfaces of *Moebius* structures, one is confronted in a more philosophically meaning with terms such as eternity and infinity, which always presuppose a certain system stability. In practice, a twisted *Moebius* conveyer belt makes equal wear amounts possible due to the use of the entire surface area of the belt [12].

Last but not least and more practical, the golden quartic may also be important in the field of life coding [13] and in quantum information science [14].

This contribution can be understood as a supplement and continuation of an already published work of the present author [13] reviewing also some earlier published work. However, he well knows that objective truth is a continually evolving matter of science. Human beings are only able to approximate the truth, and cherished truths have to be thrown overboard from time to time. The article of *Nobel* laureate *Franc Wilczek* about the enigmatic electron may bring this verity to the point [15].

2. Reciprocity, Calculus, and the Golden Ratio Sophistication

The golden ratio is the most irrational number with the simplest infinite continued fraction representation at all and a very adaptable number-theoretical chameleon. Special attention is paid to the reciprocity property of the golden ratio as effective pre-calculator of natures creativness. We use the definition

$$\varphi = \frac{\sqrt{5}-1}{2} = \frac{1}{1+\dfrac{1}{1+\dfrac{1}{1+\cdots}}} = 0.6180339887\cdots \tag{1}$$

However, the golden ratio is frequently used by others as the reciprocal of this value

$$\varphi^{-1} = 1 + \varphi = \frac{\sqrt{5}+1}{2} = 1.6180339887\cdots \tag{2}$$

Another important number, the fifth power of the golden ratio, should be considered in more detail, because it is connected to phase transitions from microscopic [16] [17] up to cosmic scale [18] [19]

$$\varphi^5 = 0.0901699\cdots = \cfrac{1}{11+\cfrac{1}{11+\cfrac{1}{11+\cdots}}} \tag{3}$$

There is another nice continued fraction approach to represent φ^{-1}

$$r = \sqrt{1+\sqrt{1+\sqrt{1+\cdots}}} = \sqrt{1+r} \tag{4}$$

giving the quadratic equation $r^2 - r - 1 = 0$ with the solution

$$r_1 = \varphi^{-1} = 1.6180339887\cdots \tag{5}$$

The infinite series expansion of the functions $\frac{1}{1-x}$ respectively $\frac{1}{1+x}$ with its simplest geometrical sequences of powers of the variable x delivers further insight into the secret of this number and its fractal nature

$$\frac{1}{1-x} = \sum_{n=0}^{\infty} x^n = 1 + x + x^2 + x^3 + x^4 + \cdots, \ |x| < 1 \tag{6}$$

Remembering, the time transformation according to the new *IRT* theory [18] resulted in this simple formula $\frac{\Delta t}{\Delta t_0} = \frac{1}{1-\beta}$, where $\beta = \frac{v}{c}$.

A special application is given for $x = \varphi$, where $\frac{1}{1-\varphi} = \varphi^{-2} = 2.6180339887\cdots$ respectively

$$\frac{1}{1-\varphi} - 1 = \varphi^{-1} = \varphi + \varphi^2 + \varphi^3 + \varphi^4 + \cdots \tag{7}$$

$$\frac{1}{1-\varphi} - 2 = \varphi = \varphi^3 + \varphi^4 + \varphi^5 + \varphi^6 + \cdots \tag{8}$$

Noticeably, the series expansion of the obverse function $\frac{1}{1+x}$ has been first described by none other than *Isaak Newton* already in 1671 [20] as special case of the general binomial series. Replacing in Equation (2) x by $-x$ or specialize the binomial series for arbitrary rational values of n

$$(1+x)^n = 1 + nx + \frac{n(n-1)}{2!}x^2 + \frac{n(n-1)(n-2)}{3!}x^3 + \cdots \tag{9}$$

one gets for $n = -1$ a series with terms of alternating signs

$$\frac{1}{1+x} = 1 - x + x^2 - x^3 + x^4 - \cdots \tag{10}$$

Again one can replace x by φ and get the result, albeit a trivial one (see also Equation (4))

$$\frac{1}{1+\varphi} = \varphi = 1-\varphi+\varphi^2-\varphi^3+\varphi^4-\cdots = \varphi \tag{11}$$

It seems as if a snake is biting its tail. The series expansion allows an insight into the fractal nature of these relations and its close proximity to *Newton*'s "calculus as an algebraic analogue of arithmetic with infinite decimals", quoting the reflection of *Stillwell* [21]. On can also state a scientific contiguity to *El Naschie*'s ε-Infinity Theory [19] as well as to the *Feynman* diagrams in quantum electrodynamics, following *Feynman*'s honestly excellent *Nobel* lecture [22] [23].

Application of such polynomial approximations is utilized by a new relativistic nuclear fusion approach of the present author based on the *Information Relativity Theory* [18]. Furthermore, the relationship to double-well structures and its connection to quantum information research is considered as a fascinating scientific field [13] [14].

3. Beyond Chiral Platonic Solids Showing Golden Ratio Geometry

Two simple dual platonic solids continue to fascinate mathematicians, crystallograsphers, physicists as well as biologist, because nature likes obviously a combination of sixfold with fivefold symmetry. In times of an ongoing viral pandemic, we are confronted with the highly effective packaging and transportation of genetic information within the envelope (capside) of an icosahedron and its unwrapping to produce fatal effects in the human body. The dense packing of equal spheres (atom clustering), for instance with *Fibonacci* numbers 13 and 55, has been studied by *Mackay*, where a central sphere is repeatedly surrounded by n layers of icosahedral shells [24]. In the following we want to deals with the regular icosahedron besides its dual solid, the regular pentagonal dodecahedron, belonging to the five platonic solids. We discard centrosymmetry and focus on chiral *I532* rotation symmetry of order 60 (**Figure 1**).

Left: Regular icosahedron projected about down a threefold axis, composed of 20 equilateral triangles, 12 vertices and 30 edges. Right: Regular pentagonal dodecahedron, composed of 12 equilateral pentagons, 20 vertices and 30 edges. Coordinates of vertices see **Appendix A.1**.

Remarkably, the ratio of the in-sphere volume V_{sph} to the polyhedron volume V_p of the icosahedron shows *Fibonacci* number 13 as an approximation in the relation [25] (see also **Appendix A.1**)

$$\frac{V_{sph}}{V_p} = \pi \cdot \frac{\varphi^{-4}}{15\sqrt{3}} \approx \frac{\pi}{2 \cdot 13}\varphi^{-4} \tag{12}$$

The icosahedron can be represented by algebraic equations that map for instance the positions of its vertices respectively face centers using projective geometry. A stereographic projection of the vertices of an icosahedron with unit

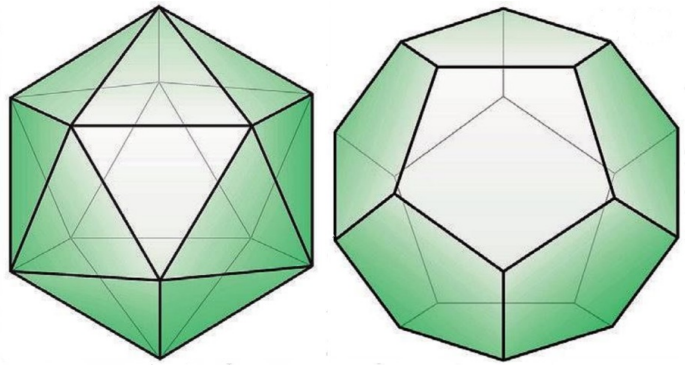

Figure 1. Projection of dual platonic solids.

circumradius from the south pole of its circumsphere onto the plane $z = 0$ delivers the simplest equation [26] [27] [28] [29]

$$(z,1) = z\left(z^{10} + 11z^5 - 1\right) = 0 \tag{13}$$

The projection of the face centers of this solid with unit in-radius onto a complex plane resulted in the equation

$$H(z,1) = z^{20} - 228z^{15} + 494z^{10} + 228z^5 + 1 \tag{14}$$

In this case the roots accordingly correspond to the locations of the face midpoints on the *Riemann* sphere. Interestingly but not surprisingly, the coefficient ratio yields 494/228 = 13/6 and contains again the *Fibonacci* numerator 13. The coefficients 228 as well as 494 can be replaced by a golden mean based approximation besides number 13

$$228 \approx \frac{4}{3}\left(13 + \frac{\varphi^4}{\sqrt{3+\varphi}}\right)^2 = 228.00022 \tag{15}$$

$$228 \approx \frac{4}{3}\left(13 + \frac{1}{13}\right)^2 = 228.00789 \tag{16}$$

$$494 \approx \frac{2}{9}\cdot 13\left(13 + \frac{1}{13}\right)^2 = 494.01709 \tag{17}$$

Based on the preliminary work by *Gordon* [30], *Klein* showed the connection between the regular icosahedron, one of the five *Platonic* bodies, and the solution of the quintic polynomial. Instead of following *Klein*'s quintic icosahedral solution, the substitution of the complex variable $z^5 \to x$ formally leads to a quartic polynomial

$$H(x,1) = x^4 - 228x^3 + 494x^2 + 228x + 1 \tag{18}$$

$$\approx x^4 - \frac{4}{3}\left(13 + \frac{1}{13}\right)^2 x\left(x^2 - \frac{13}{6}x - 1\right) + 1 \tag{19}$$

The four root of this polynomial have been calculated giving

$$x_3 = -\frac{1}{x_2},\ x_4 = -\frac{1}{x_1} \tag{20}$$

$$x_3 = 2.58365 \approx 228 - \frac{4}{3}13^2 = 2.66666 \tag{21}$$

$$x_4 = 225.80782 \approx \frac{4}{3}13^2 = 225.33333 \tag{22}$$

In addition, it yields

$$\sum_{i=1}^{4} x_i = 228 \tag{23}$$

The reader is frequently confronted with *Fibonacci* number 13, which obviously plays an important role besides φ and φ^5 when assessing bio-coding and related storage and processing of information. In the following we will work with another quartic polynomial and with coefficients like number 228 just considered.

4. Golden Quartic Polynomial Approach

The minimal polynomial of the golden ratio respectively its uneven powers (proof was reported by [31]) is given by

$$x^2 - ax - 1 = 0 \tag{24}$$

where $a = L_{2n} = \{1, 4, 11, 29, \cdots\}$ represents the series of even *Lucas* numbers [32]. The two roots of this polynomial are $x_1 = \varphi^{-(n-1)}$ and $x_2 = -\varphi^{n-1}$. The L_n number series $L_n = \{2, 1, 3, 4, 7, 11, 18, 29, \cdots\}$ was named after the *French* mathematician *François Édouard Anatole Lucas* (1842-1891) [32].

Now we introduce a simple approach to decompose important numbers such as number 137 using the following relation, which has been recently applied by the present author [13]

$$a\left(x + x^{-1}\right)^2 = n \tag{25}$$

This approach can be recast in the depressed quartic polynomial equation exhibiting a symmetrical double-well structure (see **Figure 2**)

$$x^4 - \left(\frac{n}{a} - 2\right)x^2 + 1 = 0 \tag{26}$$

The roots for the quartic can easily be calculated by the relation

$$x_i = \pm\sqrt{\frac{n}{2a} - 1 \pm \sqrt{\left(\frac{n}{2a} - 1\right)^2 - 1}} \tag{27}$$

indicating that $x_{3,4} = \pm x_1^{-1}$. Full quartic polynomials can be fortunately solved by applying the procedure given recently by *Tehrani* [33].

Exemplarily, for $n = 5$, $a = 1$ we are confronted with the golden mean as roots of the quartic

$$x_{1,2} = \pm\varphi^{-1} = \pm 1.6180339887\cdots, \quad x_{3,4} = \pm\varphi = \pm 0.6180339887\cdots$$

and for $n = 9$, $a = 1$ it yields the second power of the golden mean

$$x_{1,2} = \pm\varphi^{-2} = \pm 2.6180339887\cdots, \quad x_{3,4} = \pm\varphi^2 = \pm 0.38196601\cdots \tag{28}$$

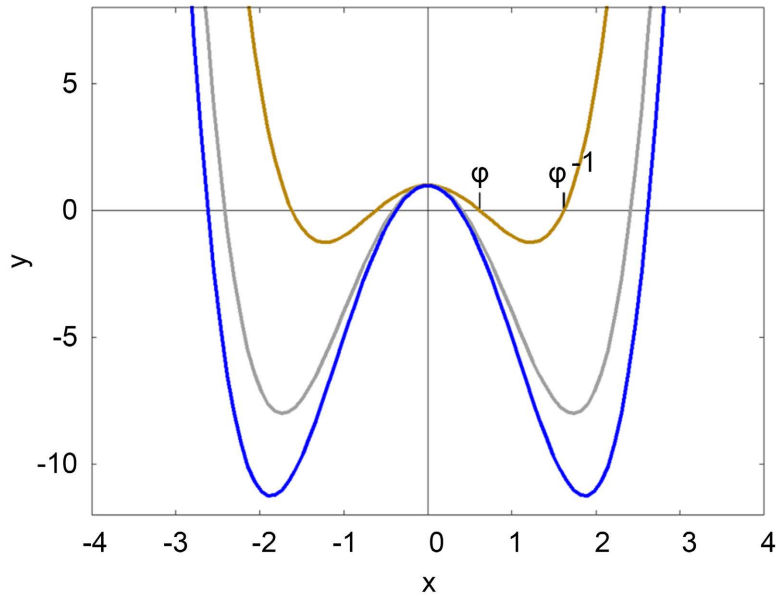

Figure 2. Quartic double-well polynomial according to equation (26), depicted for $n = 5$ (golden), 8 (silver) and 9 (blue).

More generally, the numbers series connected with golden ratio powers can be expressed by *Lucas* numbers $L_{2n+1} = \{3, 7, 18, 47, 123, \cdots\}$ according to

$$\left(\varphi^n + \varphi^{-n}\right)^2 = L_{2n+1} + 2 \tag{29}$$

Because of the intimate connection with the golden ratio the name golden quartic polynomial was introduced by the present author.

Besides this number series, as a trivial result, numbers that are well approximated to an integer can be generated for $n = m^2 + 2$. For instance, $n = 13^2 + 2 = 171 = \frac{3}{4}228$ delivers the solution $x_1 = 12.999777$. Selected solutions are presented in **Table 1**.

Therefore, this simple quartic is a very interesting one when we are dealing with the prerequisites of life and related matter governed by the golden mean or when we discuss possibilities of information processing. In the next chapter we apply the golden quartic polynomial to analyze fundamental numbers that are connected with the electron.

Very recently, the present author became aware about contributions by *McMullin* [34] as well as by *Totland* dealing with quartic polynomials in context with the golden ratio [35]. Also *Penn* demonstrated by an interesting *YouTube* contribution that every quartic polynomial is golden [36].

5. Beyond Number 137

Number 137 is not a mystic one, but is connected with the reciprocal of *Sommerfeld*'s fine-structure constant α and this way connected with the electron [37]. The fine-structure constant α describes the coupling respectively measure of the strength of the electromagnetic force that determines the interaction between

Table 1. Selected solutions for the quartic polynomial equation $x^4-(n-2)x^2+1=0$.

n		$\sqrt{n}=x_1+x_1^{-1}$	notation	x_1	notation	x_1^{-1}
4		2	φ^0	1	φ^0	1
5		$\sqrt{5}$	φ^{-1}	1.6180339887	φ	0.6180339887
8		$2\cdot\sqrt{2}$	δ_s^{-1}	2.4142135623	δ_s	0.414213562
9		3	φ^{-2}	2.6180339887	φ^2	0.381966011
18	4^2+2	$3\cdot\sqrt{2}$		3.9921490369		
20		$2\cdot\sqrt{5}$	φ^{-3}	4.2360679774	φ^3	0.236067977
27	5^2+2			4.9959919730		
32		$4\cdot\sqrt{2}$		5.4741784358		0.1826758136
38	6^2+2			5.9976829489		
49		7	φ^{-4}	6.8541019662	φ^4	0.1458980337
51	7^2+2			6.9985415144		
66	8^2+2			7.9990231393		
83	9^2+2			8.9993139982		
102	10^2+2			9.9994999374		
123	11^2+2			10.999624310		
125		$5\cdot\sqrt{5}$	φ^{-5}	11.090169943	φ^5	0.090169943
146	12^2+2			11.999710630		
171	13^2+2			12.999772406		

φ golden mean, δ_s silver mean.

electrically charged elementary particles (electron) and photons (light). This coupling is given by the relation

$$\alpha=\frac{1}{4\pi\epsilon_0}\cdot\frac{e^2}{\bar{h}c} \tag{30}$$

where e is the elementary charge of the electron, ϵ_0 is the permittivity of the vacuum, $\bar{h}$ is the reduced *Planck* constant, and c is the speed of light. The precisely determined *CODATA* value is [38]

$$\alpha=7.2973525693(11)\times10^{-3} \tag{31}$$

Its reciprocal gets

$$\alpha^{-1}=137.035999084(21) \tag{32}$$

The stability of a chemical element with atomic number Z is governed by the factor $\sqrt{1-(\alpha Z)^2}$ in the energy expression. Therefore, $Z=137$ should be the limit for the periodic table of elements [22] [39]. At the moment, the man-made heaviest element in terms of the atomic weight is $_{118}$Og (oganesson), recovered by *Y. T. Oganessian* in 2002 [40].

Recently, *Sherbon* presented a highly recommendable contribution about the golden ratio geometry and the fine-structure constant based on the solution of a general quartic polynomial with integer coefficients [41]

$$x^4 - 137x^3 - 10x^2 + 697x - 365 = 0 \tag{33}$$

The solution $x_1 = 137.035999168$ would approximate the value of α^{-1} very precisely. Again we recommend the new approach of *Tehrani* to solve such a quartic [33].

However, the actual sequence of matching decimals may not be requested due to the ongoing correction of the physical theory of the electron. Instead, we use a less precise golden mean corrected approximation of the form [42]

$$137 + \frac{2}{5}\varphi^5 = 137.0360679\cdots \tag{34}$$

Also the fractal part of π can be well approximated with the aid of the reciprocal of *Sommerfeld*'s fine structure constant [42]

$$\pi - 3 = 0.14159265\cdots \approx \frac{16}{137-24} = 0.14159292\cdots \tag{35}$$

Vice versa, 137 can simply be approximated by π combined with small *Fibonacci* numbers [42]

$$137 \approx 8\cdot\left(3 + \frac{2}{\pi - 3}\right) = 137.0002129\cdots \tag{36}$$

Interestingly, for number n = 137 and a = 1, the roots of the golden quartic polynomial (Equation (21)) resulted in $x_{1,2} = \pm 11.61863$ near $11+\varphi$ and $x_{3,4} = \pm x_{1,2}^{-1} = \pm 0.086068$. If one uses the exact value of $11+\varphi$, then one gets

$$\left(11 + \varphi + \frac{1}{11+\varphi}\right)^2 = 136.9861\cdots \approx 137 \tag{37}$$

However, if one tentatively chooses $n = 137.0360$ (inverse fine-structure constant), the result for the roots is

$$x_{1,2} = \pm 11.620186\cdots,\ x_{3,4} = \pm x_1^{-1} = \pm 0.086057\cdots \tag{38}$$

Interestingly, adding to the value of $11+\varphi$ the value of the gyromagnetic correction factor of the electron, $\Delta g_e = 0.00231878$ (see **Chapter 6**), we get almost the inverse fine-structure constant

$$\left(11 + \varphi + \Delta g_e + \frac{1}{11+\varphi+\Delta g_e}\right)^2 = 137.040002 \tag{39}$$

In a previously given contribution [13] we have examined the coefficients of the icosahedron equation in a similar way as given above. Using the coefficient 228 we found

$$\frac{4}{3}\left(x + x^{-1}\right)^2 = 228 \tag{40}$$

which can be recast into the quadric polynomial equation

$$x^4 - 169x^2 + 1 = x^4 - (13x)^2 + 1 = 0 \tag{41}$$

with solutions $x_{1,2} = \pm 12.99977241 \approx \pm 13$ and $x_{3,4} = \pm x_1^{-1} = \pm 0.076924423$.

Furthermore, one can couple number 228 with α^{-1} respectively number 137 by the relation

$$\frac{3}{5}228 + \varphi^3 = 136.8 + 0.236067976 = 137.0360\cdots \tag{42}$$

because it yields (compare Equation (3))

$$\varphi^3 = \frac{2}{5}\varphi^5 + \frac{1}{5} \tag{43}$$

One obtains a slightly larger value using the integer number 13

$$\frac{4}{5}\left(13 + \frac{1}{13}\right)^2 + \varphi^3 = 136.8047\cdots + \varphi^3 = 137.0407\cdots \tag{44}$$

The other coefficient of the icosahedron equation is number 494. When working with this number, we obtain again

$$\frac{6}{13}\cdot\frac{3}{5}\cdot 494 = 136.8 + \varphi^3 = 137.0360\cdots \tag{45}$$

Finally, from the *Kummer* surface approach, applied to the *DNA* genetic code algebraic interpretation [44] [45], we extract the number 1368 and find again

$$\frac{1}{6}\cdot\frac{3}{5}\cdot 1368 = 136.8 + \varphi^3 = 137.0360\cdots \tag{46}$$

In this way, coefficients of the icosahedron equation or numbers connected with the *Kummer* surface can traced back to the number 137 respectively the inverse fine-structure constant. All numerical findings point towards an intimate connection of electron's quantum vortex structure near an icosahedron shape.

A puzzle points to the importance of geometrical relations. *Bowen and Mulkern* [4] reported about a relation between the *Compto*n radius of the electron r_c, the *Bohr* radius of the first electron orbit in the hydrogen atom r_B, and the fine-structure constant α, possibly caused by electron's photon absorption ability

$$\frac{r_c}{r_B} = \frac{3.86159246\times 10^{-13}}{5.2917721092\times 10^{-11}} = 0.0072973522 = \alpha \tag{47}$$

6. The Gyromagnetic Correction Factor of the Electron

Now we turn to the gyromagnetic correction factor of the electron. The g_e factor of the electron, conceived as a classical charged particle, is determined by the relation

$$\vec{\mu} = g_e \mu_B \frac{\vec{S}}{\hbar},\ \mu_B = \frac{e}{2m} \tag{48}$$

where $\vec{\mu}$ is the observable magnetic moment, μ_B is the *Bohr* magneton, and $\vec{S}$ is the spin of the electron, e respectively m are charge respectively mass of

the electron, and $\bar{h}$ is the reduced *Planck* constant.

However, the spin as half-integer quantum number of the electron was introduced without any physical justification [46]. Recently, a first attempt has been undertaken by He *et al.* [47] to connect the golden mean with the ad hoc spin-1/2 construct. Such golden mean approach may be the result of dark halo movement around the stretched electron in the sense of the *Information Relativity* theory.

Remembering that the "anomalous part" of the gyromagnetic factor Δg_e was recently given by a simple golden mean representation with sufficient accuracy [48]

$$\Delta g_e = \ln\left(1+\frac{\varphi^6}{24}\right) = 0.002319312\cdots \tag{49}$$

while a series expansion yields a value more accurate up to the tenth decimal place

$$\Delta g_e = \frac{\varphi^6}{24} - \frac{1}{2}\left(\frac{\varphi^6}{24}\right)^2 - \frac{1}{4}\left(\frac{\varphi^6}{24}\right)^3 = 0.002319304\cdots \tag{50}$$

In this previous publication the present author did not connect the result with any icosahedral structure of the electron, but number 24 in the denominator was a strong indicator of what is being deduced in the following chapters.

The result may be compared to the high accuracy of the best known experimental value for g_e determined as one-electron cyclotron transition for an electron trapped in an electrostatic quadrupol potential (*Penning* trap) [49] [50]

$$g_e = 2.00231930436182(52) \tag{51}$$

In a seminal idea of He *et al.* [47] the spin quantum number s in the spin momentum term $\frac{\vec{S}}{\bar{h}} = \sqrt{s(1+s)}$ was replaced by a quantized golden mean $\tilde{\varphi}$ giving

$$\frac{g_e}{2} = \sqrt{\tilde{\varphi}(1+\tilde{\varphi})} \tag{52}$$

A special infinitely continued fraction based on the golden mean was some years ago introduced by the present author with a $\tilde{\varphi}$ sibling of the golden mean [42] [51]

$$\tilde{\varphi} = \frac{\sqrt{5+\delta}-1}{2} = \cfrac{1}{1-\delta_1+\cfrac{1}{1-\delta_1+\cfrac{1}{1-\delta_1+\cdots}}} \tag{53}$$

The calculation with $\delta_1 = 0.00374774 \approx \frac{1}{266.\overline{6}}\cdots \approx \delta/\varphi \approx \frac{\varphi^5}{4!}$ yielded $\tilde{\varphi} = 0.619071099$. One may speak of a nested golden mean based continued fraction. The value $\tilde{\varphi}$ represents the quantized golden mean in our theory of the gyromagnetic factor of the electron without using the half-spin theory

$$g_e = 2 \cdot \sqrt{\tilde{\varphi} \cdot (1 + \tilde{\varphi})} = 2.00231878 \tag{54}$$

The number $266.\overline{6}$ is very interesting. The division by integers frequently delivers numbers with repeating decimals, exemplified by $266.\overline{6}/24 = 11.\overline{1}$ [42].

In the following chapter, we develop an idea about the vortex structure of the electron and consequences for its anomalous *g*-factor as indicator for such structure.

7. Proposed Quantum Vortex Structure of the Electron

The photon may be considered as being composed of two partial waves, where a normal part is accompanied by a "dark" pilot wave of opposite chirality. The photon model of *Gauthier* [2] supposes that such dipole entity intrinsically formed from two helical strands of opposite chirality and charge is stable. When the oppositely charged strands are separated, both simultaneously formed particles move away from each other quickly due to their magnetic repulsion, even excessing their enormous electrostatic attraction. The magnetic force and electrostatic force would balance each other out at a distance of r_0 (see **Appendix A.2**)

$$r_0 = \frac{\sqrt{3}}{2} r_c = 3.344237 \times 10^{-13} \text{ m} \tag{55}$$

Therefore, electron and positron already suffer a strong mutual repulsion at a distance of the *Compton* radius $r_c = 3.8615926 \times 10^{-13}$ m, the smallest physically plausible distance. So they can exist long time as quite stable fermionic entities, because perturbation would require additional energies as high as the added up matter-energy of both sister particles (pair destruction).

Using the before worked out results we present new ideas about the possible structure of the electron assuming an energetic surface or quantum vortex structure inscribed in a regular icosahedron or its dual polyhedron (regular pentagonal dodecahedron), combining our presented results of number theory with the idea of a parent photon exhibiting a double-helical structure composed of two charged single-strand half-photons similar to *Gauthier*'s approach [2]. Although his idea is physically well substantiated, one should not exclude alternative approaches. A nested double helix can be a dipole keeping opposite charges at its strand ends. This is the picture of the *DNA* structure.

However, one can construct also a "double" helix of nested strands with opposite chirality, when both energy trajectories are displaced against each other by a small amount in the moving direction. The diameter of this composite would be the diameter of the helix. An elliptical twisting of the strands could possibly provide a further reduction of unwanted energetic interaction. The parametric equations for a golden elliptical helix are given in **Appendix**. When a strand of double helices with 13 half-turns (uneven *Fibonacci* number) is joined together at both ends forming a multiply screwed *Moebius* strand, and the double helix is then cut into two single strands (it requires starting from a helix struc-

ture that can be cut lengthwise), which may be again energetically favorable, it remains a vortex structure that can be arranged in such a way that the 12 turning points of the slings are placed towards the vertices of a regular icosahedron forming a *Moebius* ball (see **Figure 1**). The slings taper towards the center of the icosahedron. There is a dihedral angle of $180-\arccos\left(\frac{\sqrt{5}}{3}\right)=138.1897$ degrees between successive slings. The radius of this construct may be the in-sphere radius of an icosahedron.

However, what can we deduce from group theory? If one jumps from a vertex to the next one via a chord, arranged perpendicular to each of the 30 edges and corresponding to the edges of the dual solid, one can't reach all 12 vertices in a single turn. Decomposing the order 60 of the group *I532* into $5\times 12 \text{ vertices} = 3\times 20 \text{ faces} = 2\times 30 \text{ edges}$ tells us that we need at least 5 turns reaching the starting vertex point in a "helical" sequence. So electron's vortex structure is indeed a labyrinth, from which escape is hardly possible unless by an external high energy impact, like the forever bound ferryman in a German fairy tale.

The motion profile can better be understood, if the icosahedron is unfolded onto a plane like a paper model, following the "spiraling" pattern on the formed hexagonal net of triangles.

The mirrored structures of the sister particles will certainly influence each other at the very beginning of formation, inscribing the opposed chiral revolving. We can learn more about a possible double helix unzipping mechanism from our knowledge about the *DNA* replication process.

Furthermore, when combining *Sommerfeld*'s fine-structure constant α with the golden mean φ, one can approximate number 13 once more

$$\sqrt{2\varphi/\alpha}=13.01482999\cdots \tag{56}$$

Using this result, one can relate the electric charge Q of *Gauthier*'s double helix photon dipole model in relation to the elementary charge e of the electron

$$Q\cdot\sqrt{\varphi}=\pm 13.01483\cdot e\approx\pm 13\cdot e \tag{57}$$

Surprisingly, considering Q spread over 13 half-turns, on gets per half-turn a charge of

$$\frac{Q\cdot\sqrt{\varphi}}{13}\approx\pm e \tag{58}$$

Interestingly, in the proton structure the down quark has a charge of $-13e$.

The length l_0 of a single turn of a helix having height z_0 and radius r_0 can be calculated by unrolling the helix to a plane and then applying the *Pythagorean* theorem

$$l_0=\sqrt{z_0^2+4\pi^2 r_0^2} \tag{59}$$

This step was obviously not considered in the theory of *Bowen* [4] [5].

If we identify z_0 with the *Compton* wavelength $\lambda_c = \frac{h}{m_e c}$ and r_0 with $\lambda_c/4\pi$ according to [2], we get for l_0

$$l_0 = \sqrt{\lambda_c^2 + \frac{1}{4}\lambda_c^2} = \frac{\lambda_c}{2}\sqrt{5} = \left(\varphi + \frac{1}{2}\right)\lambda_c \tag{60}$$

The term $\sqrt{5}$ indicates for the first time that the golden ratio is involved. Now, the entire length of $13 \cdot l_0$ must be compacted into a 12-sling *Moebius* ball to find its radius. The length of a single sling yields

$$l_{sling} = \frac{13}{24}\sqrt{5} \cdot \lambda_c = 1.21120 \cdot \lambda_c \approx \frac{6}{5} \cdot \lambda_c \tag{61}$$

and the radius of a sling, representing the radius of the *Moebius* ball, would be

$$r_{sling} = \frac{l_{sling}}{2\pi} \cdot \sqrt{2/3} \approx r_c \tag{62}$$

The factor $\sqrt{\sin(138.1897)} = \sqrt{2/3}$ takes into account the dihedral angle relation between two consecutive slings. Interestingly, the factor $\frac{r_c}{r_{sling}} = 1.011180106$ can be compared with the integrated charge relation on a *Moebius* strip with unit stripe width and charge density (see **Appendix A.5**).

Remarkably, by using the in-sphere radius of an icosahedron (see also **Appendix A.1**), the edge length of the icosahedral cage then gives

$$a_{icos} = \frac{13}{24}\sqrt{5} \cdot \sqrt{2/3} \cdot 2\sqrt{3} \cdot \varphi^2 \cdot r_c = 1.308539 \cdot r_c \approx \frac{\varphi^{-2}}{2} \cdot r_c \tag{63}$$

In this way, a self-confined chiral ball structure with about the *Compton* radius $r_c \approx 3.86 \times 10^{-13}$ m is generated that did not forgot where it was originating from. It remains to be shown, whether all the properties of the fundamental particle named electron can be confirmed as a self-stabilizing dynamic system that does not radiate. Once again it may be noticed that the icosahedron picture couples the structure with the golden ratio in harmony with what nature would expect.

However, for the electron instead of an icosahedron also the regular dodecahedron as its dual polyhedron can be chosen as confining cage. Then, these slings would hit the 12 face midpoints. If one operates with the next higher uneven *Fibonacci* number 21, the procedure given above would deliver 20 slings, which would be directed towards the face midpoints of the regular icosahedron, or to the vertices of the dodecahedron. We notice that the vortex structure of the electron and the parametric equations of a *Horn* torus given by *Gauthier* are also quite similar to these of a *Moebius* curve (see **Appendix A.4**) [2]. Nevertheless, his elegantly worked out physical interpretation can be transferred with few changes to our vortex construct.

With respect to the gyromagnetic correction factor of the electron Δg_e, also an icosahedron based numerical interpretation can be found, combining the Equation (44) with terms from the icosahedron Equation (14) respectively the golden

quartic polynomial (see last line of Table 1), and the circumsphere radius r_{circ} of an icosahedron with unit triangle edge length [13] [25]

$$\Delta g_e \approx \frac{\varphi^6}{24} \approx \frac{5}{3} \cdot \frac{\sqrt{3+\varphi}}{8 \cdot \left(13+\frac{1}{13}\right)^2} \approx \frac{5}{9} \cdot \frac{r_{circ}}{228} = 0.0023174 \tag{64}$$

where $r_{circ} = \frac{\sqrt{3+\varphi}}{2}$ (see **Appendix A.1**). However, when using a power of the ratio of 12 slings to 13 half-turns, another numerical relation for the anomalous part of the electron can by derived (see **Appendix A.5**)

$$\Delta g_e \approx \left(\frac{12}{13}\right)^{3/2} \cdot \frac{1}{\sqrt{5} \cdot \left(13+\frac{1}{13}\right)^2} = 0.0023193\cdots \tag{65}$$

Alternatively, turning back to *Schwinger*'s classical and simple *QED* approximation for the anomalous part of the *g*-factor as α/π [52], we can apply a modified $\tilde{\pi} > \pi$ as result of the *Moebius* stripe charge calculation according to Equation (108) (see **Appendix A.5**), but modified for the more complex *Moebius* ball structure. We can possibly verify a value of $\tilde{\pi} = 3.146644586$ ($2\tilde{\pi} = 6.293289178$). Thereby we would be able to confirm the experimental Δg_e that has been reduced by *IRT* mass correction giving [18] [42]

$$\Delta g_e = \alpha/\tilde{\pi} = 0.00231909 \tag{66}$$

It would provide a plausible physical understanding of such purely geometric icosahedron-based relationships, beyond *Feynman*'s approach [53], connecting the anomalous *g*-factor little larger than 2 to the chaotic vortex motion of the electron. If the charge would reside on the surface of the ball, a *g*-factor of only 5/3 results [5]. However, if the electron charge is spread along the striped inner structure of the chiral *Moebius* ball, we should be able to prove by fortune the true anomalous *g*-factor in full glory from its chiral asymmetry at one fell swoop. The next task is to find an analytical expression for the chaotic motion along multiple *Moebius* stripes with forced icosahedral symmetry and proceed according to the total charge approach given in **Appendix A.5**. The exorbitantly accurate determined experimental value Δg_e will make it easier to choose a very reliable structural electron model. Then we can unravel structurally the spin-orbital separation of the electron in quasi 1D *Mott*-insulators, too [54]. When the time is ripe, we will have learnt whether the structure of the electron is a fundamental one and that the "anomalous" *g*-factor may be more simply as thought and unequivocally a universal constant. Also the electron spin construct [46] becomes a new meaning without losing its practical importance. The mathematics behind a *Horn* torus [2] [4] [6] [55] in relation to the *Moebius* ball can help to judge differently proposed electron structures. A dynamic visualization is in progress.

8. Superconducting Strands

There are indications that both conventional as well as unconventional super-

conductivity is basically governed by hole-carriers, which are guided without resistance in a reversible way through the lattice [56] [57] [58]. When asking, what the structure of delocalized hole-carriers in the superconducting state would be, as all-convincing test case of our approach, the assumed chiral *Moebius* stripe governed property of the single electron could be relevant.

A delocalized electron hole may also be portrayed by a helical strand able to transport positive charge. During the unfolding of involved delocalizing *Moebius* electron balls a nested double-helical wavy entity of equal strand chirality (*DNA* case) could be formed, which can easily be unzipped just above the superconducting transition temperature T_c and compacted again into two separated "particles". In this way the equi-chiral *wavy* entity is different to the photon, composed of two half-photons of opposed chirality and charge. The mathematical and experimental verification should be a worthwhile task for future cooperation.

In addition, the reader may study a seminal contribution by *Schiller* about tangled strands, elementary particles and the fine-structure constant [59].

Remembering, the present author suggested linking the optimum hole doping σ_0 of high-T_c superconductors with the golden mean in the form of *Hardy*'s maximum quantum probability of two particles [17] [56] and presented the connection with number 13

$$\sigma_0 \approx \frac{8}{\pi}\varphi^5 = 0.2293 \approx \frac{3}{13} \tag{67}$$

Obviously, this optimum is near a quantum critical point in the phase diagram. In addition, the relation of the *Fermi* speed v_F to the *Klitzing* speed v_K comes out as

$$\frac{v_F}{v_K} \approx \frac{2}{\pi}\varphi^5 = 0.0571 \approx \frac{3}{4\times 13} \tag{68}$$

Both relations document the fractal nature of the electronic response in superconductors. It was suggested recently that the same is true for conventional superconductors [56]. Also *Prester* had reported before about evidence of a fractal dissipative regime in high-T_c superconductors [60].

9. Challenge for Modeling of Inorganic or Organic Moebius Ball Structures

We pose the question whether it could be possible to synthesize an inorganic or organic compound having the structure of the proposed *Moebius* ball. In 2003, niobium selenide $NbSe_3$ could be designed with the morphology of a *Moebius* stripe by combining chemical transport reactions with template technique [61]. Very recently, *Moebius* stripes of chiral block copolymers were synthesized via a fast self-assembly of block copolymer polystyrene-block-poly(D-lactide acid) (PS-b-PDLA) in tetrahydrofuran – water mixed solvents [62]. The spontaneous formation of such chiral structures and possibly that of *Moebius* ball structures

would also support the picture of a stable vortex structure of an electron in form of a *Moebius* ball of icosahedral symmetry. Organic self-assembled nanotoroids have been already synthesized with controlled helicity [63]. Some years ago, the present author reported about the possibility to synthesize a cubic antiferromagnetic cuprate super-cage composed of corner-sharing cuprate stripes [64]. We still hope for the creativeness of nanotechnology researchers and new experimental methods. Tubulin-like structures or *Moebius*-ball-like ones, simulating nature's beautiful and effective creations, are recommended for quantum information purposes including the development of quantum computers.

By the way, what could we expect from an experiment where electric current flows through an icosahedral wiring of *Moebius* loops that exemplifies a fanned coil? Perhaps it could be prepared in miniature by $3D$ printing technique.

10. Conclusion

This contribution may once more promote understanding of the relationship between number theory, topology and physical properties with the focus on the ever-present golden ratio to decipher the fractal nature of such relations. Also *Fibonacci* number 13 is a constant companion in our discussion. Starting from a golden quartic polynomial, first ever we deduce the possible structure of the elementary particle electron as a vortex construct in form of an icosahedral-shaped chiral *Moebius* ball with a radius little more than the *Compton* radius r_c. It is a beautiful geometric structure composed of 12 single-strand slings in chaotic motion, even when it would not be connected to an elementary particle. The *Moebius* ball vortex structure is a self-confined non-radiating charged compaction of helical structures proposed for the photon, and may be in this way a variation of the photon-electron theory of *Gauthier* with the changed supposition that the starting photon consists of two oppositely charged double helix strands in contrast to his single helix half-photon approach. Electron's icosahedron governed structure is manifested by the *Fibonacci* number quotient $\frac{3}{5} \approx \frac{137}{228} (\approx \varphi)$. The anomalous g-factor of the electron is certainly a direct consequence of its 5-turn confined-helical *Moebius* stripe twist motion. Furthermore, we posed the question: what the structure of delocalized hole-carriers could be, which may be understood as the marriage of wavy nested entities escaping in the dark near a superconducting transition? Our proposal should open the horizon to verify such structures of the hole/electron by sophisticated new physical experiments. In a mathematical as well as philosophical sense, the geometry of folded *Moebius* strands including the *Moebius* ball mediates between eternity and symmetry respectively chiral asymmetry. Even in *Escher*'s fine art work, combining mathematics with art, such *Moebius* icosahedron drawing could not be found. However, it is one of the most beautiful chiral motion profiles connecting icosahedral symmetry with analytical realities given by *Moebius* stripes and its quantitative solution a demanding task of differential geometry.

Conflicts of Interest

The author declares no conflict of interests regarding the publication of this paper.

References

[1] Gauthier, R. (2013) Transluminal Energy Quantum Models of the Photon and the Electron. In: Amoroso, R.L., Kauffman, L.H. and Rowlands, P., *The Physics of Realty*: *Space*, *Time*, *Matter*, *Cosmos*, World Scientific, Hackensack, 445-452. https://doi.org/10.1142/9789814504782_0045

[2] Gauthier, R. (2019) Quantum-Entangled Superluminal Double-Helix Photon Produces a Relativistic Superluminal Quantum-Vortex *Zitterbewegung* Electron and Positron. *IOP Conference Series*: *Journal of Physics: Conference Series*, **1251**, Article ID: 012016. https://doi.org/10.1088/1742-6596/1251/1/012016

[3] Williamson, J.G. (2019) A New Linear Theory of Light and Matter. *Journal of Physics*: *Conference Series*, **1251**, Article ID: 012050, 19 p. https://doi.org/10.1088/1742-6596/1251/1/012050

[4] Bowen, D. and Mulkern, R.V. (2015) An Electron Model Consistent with Electron-Positron Pair Production from High Energy Photon. *Journal of Modern Physics*, **6**, 1334-1342. https://doi.org/10.4236/jmp.2015.69138

[5] Bowen, D. (2016) The Real Reason Why the Electron's Bare G-Factor Is, 2 Times Classical. *Journal of Modern Physics*, **7**, 1200-1209. https://doi.org/10.4236/jmp.2016.710109

[6] Markouladis, E. and Antonidakis, E. (2022) A ½ Spin Fiber Model for the Electron. *International Journal of Physical Research*, **10**, 1-17. https://doi.org/10.14419/ijpr.v10i1.31874

[7] Starostin, E.L. and Van Der Heijden, G., H.M. (2007) The Shape of a Moebius Strip. *Nature Materials*, **6**, 563-567. https://doi.org/10.1038/nmat1929

[8] Godinho, M.H., Canejo, J.P., Feio, G. and Terenjev, E.M. (2010) Self-Winding of Helices in Plant Dendrils and Cellulose Liquid Crystalline Fibers. *Soft Matter*, **6**, 5965-5970. https://doi.org/10.1039/c0sm00427h

[9] Gerbode, S.J., Puzey, S.J., McCormick, A.G. and Mahadevan, L. (2012) How the Cucumber Tendrils Coil and Overwinds. *Science*, **337**, 1087-1091. https://doi.org/10.1126/science.1223304

[10] Olsen, S. (2006) The Golden Section: Nature's Greatest Secret. Bloomsbury, London, 64 p.

[11] Weiss, H. and Weiss, V. (2002) The Golden Mean as Coding Principle of the Brain. *Journal of Mathematics and Design*, **2**, 63-73.

[12] Alagappan, S. (2021) The Timeless Journey of the Möbius Strip. *Scientific American*.

[13] Otto, H.H. (2021) Beyond a Quartic Polynomial Modeling of the DNA Double-Helix Genetic Code. *Journal of Applied Mathematics and Physics*, **9**, 2558-2577. https://doi.org/10.4236/jamp.2021.910165

[14] Jelic, V. and Marsiglio, F. (2012) The Double Well Potential in Quantum Mechanics: A Simple Numerical Exact Formulation. *European Journal of Physics*, **33**, 1651-1666. arXiv: 1209.2521 [physics.ed.ph]. https://doi.org/10.1088/0143-0807/33/6/1651

[15] Wilczek, F. (2013) The Enigmatic Electron. *Nature*, **498**, 31-32. https://doi.org/10.1038/498031a

[16] Otto, H.H. (2020) Phase Transitions Governed by the Fifth Power of the Golden Mean and Beyond. *World Journal of Condensed Matter Physics*, **10**, 135-158. https://doi.org/10.4236/wjcmp.2020.103009

[17] Hardy, L. (1993) Nonlocality for Two Particles without Inequalities for Almost All Entangled States. *Physical Review Letters*, **71**, 1665-1668. https://doi.org/10.1103/PhysRevLett.71.1665

[18] Suleiman, R. (2019) Relativizing Newton. Nova Scientific Publisher, New York, 1-207.

[19] El Naschie, M.S. (2017) Elements of a New Set Theory Based Quantum Mechanics with Application in High Quantum Physics and Cosmology. *International Journal of High Energy Physics*, **4**, 65-74. https://doi.org/10.11648/j.ijhep.20170406.11

[20] Newton. I. (1671) Tractatus de Methodis Serierum et Fluxionum (Withdrawn from Publication Until, 1711 According to [4]).

[21] Stillwell. J.C. (1989) Infinite Series. In: *Mathematics and Its History*, Springer, New York, 118-134. https://doi.org/10.1007/978-1-4899-0007-4_9

[22] Feynman, R.P. (1965) The Development of the Space-Time View of Quantum Electrodynamics. NobelPrize.org Nobel Prize Outreach AB, 2021.

[23] Feynman, R.P. (1985) QED: The Strange Theory of Light and Matter. Princeton University Press, Princeton.

[24] Mackay, A.L. (1962) A Dense Non-Crystallographic Packing of Equal Spheres. *Acta Crystallographica*, **15**, 916-918. https://doi.org/10.1107/S0365110X6200239X

[25] Otto, H.H. (2021) Ratio of In-Sphere Volume to Polyhedron Volume of the Great Pyramid Compared to Selected Convex Polyhedral Solids. *Journal of Applied Mathematics and Physics*, **9**, 41-56. https://doi.org/10.4236/jamp.2021.91005

[26] Klein, F. (1884) Vorlesungen Über Das Ikosaeder Und Die Auflösung Der Gleichungen Vom Fünften Grad. Verlag B. G. Teubner, Leipzig.

[27] Slodowy, P. (1986) Das Ikosaeder Und Die Gleichungen Fünften Grades. In: *Arithmetik und Geometrie*, Mathematische Miniaturen, Vol. 3, Birkhäuser, Basel, 71-113. https://doi.org/10.1007/978-3-0348-5226-5_3

[28] Eschenburg, J.H. (1997) Das Ikosaeder Und Die Gleichungen, 5. Grades Nach Felix Klein. *Seminar am Mathematischen Institut der Universität Augsburg*, 8 November 1997/February 1999, 1-29.

[29] Nash, O. (2013) On Klein's Icosahedral Solution of the Quintic. *Expositiones Mathematicae*, **32**, 99-120. https://doi.org/10.1016/j.exmath.2013.09.003

[30] Gordon, P. (1878) Ueber die Auflösung der Gleichungen vom fünften Grade. *Mathematische Annalen*, **13**, 375-404. https://doi.org/10.1007/BF01447396

[31] Afzal, Q. and Afzal, F. (2018) Golden Mean and the Action of Mobius Group M. *International Journal of Mathematics and Computational Sciences*, **4**, 124-127.

[32] Lucas, E. (1891) Theorie Des Nombres. Gauthier-Villars, Paris.

[33] Tehrani, F.T. (2020) Solution to Polynomial Equations. *Applied Mathematics*, **11**, 53-66. https://doi.org/10.4236/am.2020.112006

[34] McMullin, L.O. (2004) How I Found the Golden Ratio on My CAS. *The North Carolina Association of Advanced Placement Mathematics Teachers Newsletters*, **13**, 6-7.

[35] Totland, H. (2009) Quartic Polynomials and the Golden Ratio. *Mathematics Magazine*, **82**, 197-201. https://doi.org/10.1080/0025570X.2009.11953618

[36] Penn, M. (2020) Every Quartic Is Golden. *YouTube*.

[37] Sommerfeld, A. (1919) Atombau und Spektrallinien. Friedrich Vieweg & Sohn, Braunschweig.

[38] National Institute of Standards and Technology (2018) The NIST Reference of Constants, Units and Uncertainty. National Institute of Standards and Technology, Gaitherburg.

[39] Maruani, J. (2018) The Dirac Electron and Elementary Interactions: The Gyromagnetic Factor, Fine-Structure Constant, and Gravitational Invariant: Derivations from Whole Numbers. In: Wang, Y., Thachuk, M., Krems, R. and Maruani, J., Eds., *Concepts, Methods and Application of Quantum Systems in Chemistry and Physics*, Vol. 31, Springer, Cham, 361-380. https://doi.org/10.1007/978-3-319-74582-4_19

[40] Oganessian, Y.T., *et al.* (2002) Results from the First, ^{249}Cf, ^{48}Ca Experiment. JINR Communication, Dubna.

[41] Sherbon, M.A. (2019) Golden Ratio Geometry and the Fine-Structure Constant. *Journal of Advances in Physics*, **16**, 362-368. https://doi.org/10.24297/jap.v16i1.8469

[42] Otto, H.H. (2020) Reciprocity as an Ever-Present Dual Property of Everything. *Journal of Modern Physics*, **11**, 98-121. https://doi.org/10.4236/jmp.2020.111007

[43] Pisano, L. (1202) Fibonacci's Liber Abaci (Book of Calculation). Biblioteca a Nazionale Di Firenze.

[44] Planat, M., Aschheim, R.A., Amaral, M.M., Fang, F. and Irwin, K. (2020) Complete Quantum Information in the DNA Genetic Code. *Symmetry*, **12**, Article No. 1993. https://doi.org/10.3390/sym12121993

[45] Planat, M., Chester, D., Aschheim, R., Amaral, M.M., Fang, F. and Irwin, K. (2021) Finite Groups for the Kummer Surface: The Genetic Code and a Quantum Gravity Analogy. *Quantum Reports*, **3**, 68-79. https://doi.org/10.3390/quantum3010005

[46] Uhlenbeck, G.E. and Goudsmit, S. (1926) Spinning Electrons and the Structure of Spectra. *Nature*, **117**, 264-265. https://doi.org/10.1038/117264a0

[47] He, J.H., Tian, D. and Otto, H.H. (2018) Is the Half-Integer Spin a First Level Approximation of the Golden Mean Hierarchy? *Results in Physics*, **11**, 362-363. https://doi.org/10.1016/j.rinp.2018.09.027

[48] Otto, H.H. (2017) Gyromagnetic Factor of the Free Electron: Quantum-Electrodynamical Correction Expressed Solely by the Golden Mean. *Nonlinear Science Letters* A, **8**, 413-415.

[49] Odom, B. (2004) Fully Quantum Measurement of the Electron Magnetic Momentum. Thesis, Harvard University, Cambridge, MA.

[50] Odom, B., Hanneke, D., D'Urso, B. and Gabrielse, G. (2006) New Measurements of the Electron Magnetic Moment Using a One-Electron Quantum Cyclotron. *Physical Review Letters*, **97**, Article ID: 030801. https://doi.org/10.1103/PhysRevLett.97.030801

[51] Otto, H.H. (2017) Continued Fraction Representations of Universal Numbers and Approximations. ResearchGate, Berlin, 1-7. https://www.researchgate.net/

[52] Schwinger, J. (1948) On Quantum-Electrodynamics and the Magnetic Moment of the Electron. *Physical Review*, **73**, 416-417. https://doi.org/10.1103/PhysRev.73.416

[53] Feynman, R.P., Leighton, R.B. and Sands, M. (1985) The Feynman Lectures on Physics. Vol. 3, Basic Books, New York.

[54] Schlappa, J., Wohlfeld, K., Zhou, K.J., Mourigal, M., Haverkort, M.W., Strocov, V.N., *et al.* (2012) Spin-Orbital Separation in the Quasi-One-Dimensional Mott Insulator Sr_2CuO_3. *Nature*, **485**, 82-85. https://doi.org/10.1038/nature10974

[55] Daeumler, W.W. (2006) Horn Torus and Physics, 'Geometry of Everything'. Personal Website.

[56] Otto, H.H. (2016) A Different Approach to High-T_c Superconductivity: Indication of Filamentary-Chaotic Conductance and Possible Routes to Superconductivity Above Room Temperature. *World Journal of Condensed Matter Physics*, **6**, 244-260. https://doi.org/10.4236/wjcmp.2016.63023

[57] Otto, H.H. (2019) Super-Hydrides of Lanthanum and Yttrium: On Optimal Conditions for Achieving Near Room Temperature Superconductivity. *World Journal of Condensed Matter Physics*, **9**, 22-36. https://doi.org/10.4236/wjcmp.2019.91002

[58] Hirsch, J.E. (2017) Towards an Understanding of Hole Superconductivity. In: Bussmann-Holder, A., Keller, H. and Bianconi, A., Eds., *High-Tc Copper Oxide Superconductors and Related Novel Materials*, Springer, Cham, 99-115. https://doi.org/10.1007/978-3-319-52675-1_9

[59] Schiller, Ch. (2021) From Strand Unification to the Fine Structure Constant—And All Colours. https://www.researchgate.net/

[60] Prester, M. (1999) Experimental Evidence of a Fractal Dissipative Regime in High-T_c Superconductors. *Physical Review* B, **60**, 3100-3103. https://doi.org/10.1103/PhysRevB.60.3100

[61] Patzke, G.R. (2003) Möbius Stripes of $NbSe_3$: Morphology Design and Solid State Chemistry. *Angewandte Chemie International Edition*, **42**, 972-974. https://doi.org/10.1002/anie.200390282

[62] Geng, Z., Xiong, B. Wang, L., Wang, K., Ren, M., Zhang, L. Zhu, J. and Yang, Z. (2019) Moebius Stripes of Chiral Block Copolymeres. *Nature Communications*, **10**, Article No. 4090. https://doi.org/10.1038/s41467-019-11991-3

[63] Quyang, G., Ji, L., Jiang, Y., Würthner, F. and Liu, M. (2020) Self-Assembled Möbius Strips with Controlled Helicity. *Nature Communications*, **11**, Article No. 5910. https://doi.org/10.1038/s41467-020-19683-z

[64] Otto, H.H. (2015) Modeling of a Cubic Antiferromagnetic Cuprate Super-Cage. *World Journal of Condensed Matter Physics*, **5**, 160-178. https://doi.org/10.4236/wjcmp.2015.53018

[65] Pauschenwein, G. (2004) Electrodynamics on a Möbius Strip. Diploma Thesis, Technische Universität Wien, Vienna.

Appendix

A.1. Geometric Relations for Relevant Platonic Bodies [25]

The polyhedron notation is given by the symbol $\left[p_i^{F_i} \right]$, where p is the polygon multiplicity and F is the number of faces. V_p polyhedron volume, V_{sph} in-sphere volume, A_p polyhedron surface area, A_{sph} in-sphere area, r_{circ} circumsphere radius, r_i in-sphere radius, a polygon edge length (Table A1).

Table A1. Coordinates of vertices. (Solids are centered at the origin and suitably scaled for sake of simplicity)

Edge length: $a = 2\varphi$					
Regular icosahedron			**Regular pentagonal dodecahedron**		
x	y	z	x	y	z
0	$\pm\varphi$	± 1	± 1	± 1	± 1
$\pm\varphi$	± 1	0	0	$\pm\varphi^{-1}$	$\pm\varphi$
± 1	0	$\pm\varphi$	$\pm\varphi^{-1}$	$\pm\varphi$	0

Regular Icosahedron $[3^{20}]$

$$V_p = \frac{5}{6}\varphi^{-2}a^3 \tag{69}$$

$$r_{circ} = \frac{\sqrt{3+\varphi}}{2}a \approx \frac{a}{2}\cdot\left(15-\frac{6}{\pi}\right)^{1/4} \tag{70}$$

$$r_i = \frac{\varphi^{-2}}{2\sqrt{3}}a \tag{71}$$

$$V_{sph} = \pi\cdot\frac{\varphi^{-6}}{18\sqrt{3}}a^3 \tag{72}$$

$$\frac{V_{sph}}{V_p} = \pi\cdot\frac{\varphi^{-4}}{15\sqrt{3}} = \pi\cdot 0.263814507 = 0.8287977 \approx \frac{\pi}{2\cdot 13}\varphi^{-4} \tag{73}$$

$$A_p = 5\cdot\sqrt{3}a^2 \tag{74}$$

$$A_{sph} = \pi\frac{\varphi^{-4}}{3}a^2 \tag{75}$$

$$\frac{A_{sph}}{A_p} = \pi\cdot\frac{\varphi^{-4}}{15\sqrt{3}} \approx \frac{\pi}{2\cdot 13}\varphi^{-4} \tag{76}$$

Regular Pentagonal Dodecahedron $[5^{12}]$:

$$V_p = \frac{\sqrt{5}}{2\varphi^4}a^3 = \frac{5}{2\varphi^3\left(1+\varphi^2\right)}a^3 = 7.6631188998\cdots a^3 \tag{77}$$

$$r_i = \frac{1}{2\sqrt{\sqrt{5}\varphi^5}}a = \frac{1}{2\varphi^2\cdot\sqrt{1+\varphi^2}}a = 1.113516364\cdots a \tag{78}$$

$$V_{sph} = \frac{4}{3}\pi r_i^3 = \pi\cdot 1.840893008\cdots a^3 \tag{79}$$

$$\frac{V_{sph}}{V_p} = 0.240227643 \cdot \pi = 0.754697398 \tag{80}$$

$$A_p = 3 \cdot \sqrt{5\left(5+2\sqrt{5}\right)} \cdot a^2 = \frac{15}{\varphi\sqrt{1+\varphi^2}} a^2 = 20.64572881\cdots a^2 \tag{81}$$

$$A_{sph} = 4\pi r_i^2 = \pi \frac{1}{\sqrt{5}\varphi^5} a^2 = \pi \cdot 4.9596747 \cdots a^2 \tag{82}$$

$$\frac{A_{sph}}{A_p} = 0.240227643 \cdot \pi = 0.754697398 \tag{83}$$

A.2. Balance of Magnetic and Electrostatic Forces

Solving the balance equation between magnetic force $\boldsymbol{f}_m$ and electrostatic force $\boldsymbol{f}_e$ leads to the separation r_0 between electron and positron, beyond both will quickly move away from each other. Following textbooks of physics we have to solve the relation (see also [4])

$$\boldsymbol{f}_m - \boldsymbol{f}_e = \frac{3\varepsilon_0}{4\pi}\left(\frac{\boldsymbol{m}_1\boldsymbol{m}_2}{r^4}\right) - \frac{1}{4\pi\varepsilon_0}\left(\frac{\boldsymbol{q}_1\boldsymbol{q}_2}{r^2}\right) = 0 \tag{84}$$

or for short

$$\frac{a}{r^4} - \frac{b}{r^2} = 0 \tag{85}$$

The solution is simply

$$r_0 = \sqrt{\frac{a}{b}} \tag{86}$$

Replacing the actual quantities yields

$$r_0 = \frac{\sqrt{3}}{4\pi}\frac{h}{m_e c} = \frac{\sqrt{3}}{2} r_c \tag{87}$$

where h is *Planck*'s constant, m_e is the mass of the electron, r_c is the *Compton* radius and $c^2\varepsilon_0\mu_0 = 1$ (*Maxwell* relation), connecting the speed of light c with the permittivity ε_0 respectively the permeability μ_0 of free space.

A.3. Parametric Equations of a Golden-Elliptical Helix

We want to construct a golden-elliptical helix by using different radii a and b that meet the condition $a = \varphi \cdot b$. The equation and coordinates are given by

$$\frac{r^2}{a^2} + \frac{z^2}{b^2} = 1 \tag{88}$$

$$x = a\sqrt{1-\frac{c^2t^2}{b^2}}\cos(t) = \varphi\sqrt{b^2 - c^2t^2}\cos(t) \tag{89}$$

$$y = a\sqrt{1-\frac{c^2t^2}{b^2}}\sin(t) = \varphi\sqrt{b^2 - c^2t^2}\sin(t) \tag{90}$$

$$z = c \cdot t \tag{91}$$

A.4. Parametrization of a Single Moebius Strip Centered at the Origin

$$x(u,t)=\left(1+t\cdot\cos\left(\frac{u}{2}\right)\right)\cos(u) \tag{92}$$

$$y(u,t)=\left(1+t\cdot\cos\left(\frac{u}{2}\right)\right)\sin(u) \tag{93}$$

$$z(u,t)=t\cdot\sin\left(\frac{u}{2}\right) \tag{94}$$

with $0\le u<2\pi$; $-l\le t\le l$.

A.5. Total Charge on a Moebius Stripe

Following *Pauschenwein*'s electrodynamics considerations about the *Moebius* strip [65], one can relate the charge Q of an area A as the integral over the area charge density σ by

$$Q(l)=\int\sigma\mathrm{d}O=\int_0^{2\pi}\int_{-l}^{l}\sigma|\boldsymbol{n}|\mathrm{d}t\mathrm{d}u \tag{95}$$

where $\boldsymbol{n}$ is the normal vector on every point of the strip. Applying the parametrization of a single *Moebius* strip, it yields for this vector $\boldsymbol{n}$ as vector product of the derivations $\boldsymbol{m}_u$ and $\boldsymbol{m}_t$

$$\boldsymbol{n}=\boldsymbol{m}_u\times\boldsymbol{m}_t \tag{96}$$

$$m_u(x)=-\left(t\cdot\cos\left(\frac{u}{2}\right)+1\right)\cdot\sin(u)-t\cdot\sin\left(\frac{u}{2}\right)\cos(u)/2 \tag{97}$$

$$m_u(y)=\left(t\cdot\cos\left(\frac{u}{2}\right)+1\right)\cdot\cos(u)-t\cdot\sin\left(\frac{u}{2}\right)\sin(u)/2 \tag{98}$$

$$m_u(z)=\frac{1}{2}t\cdot\cos\left(\frac{u}{2}\right) \tag{99}$$

$$m_t(x)=\cos\left(\frac{u}{2}\right)\cos(u) \tag{100}$$

$$m_t(y)=\cos\left(\frac{u}{2}\right)\sin(u) \tag{101}$$

$$m_t(z)=\sin\left(\frac{u}{2}\right) \tag{102}$$

$$\begin{aligned}n_x=&\sin\left(\frac{u}{2}\right)\left(\cos(u)\left(t\cdot\cos\left(\frac{u}{2}\right)+1\right)-\frac{t}{2}\sin\left(\frac{u}{2}\right)\sin(u)\right)\\&-\frac{t}{2}\cos^2\left(\frac{u}{2}\right)\sin(u)\end{aligned} \tag{103}$$

$$\begin{aligned}n_y=&\sin\left(\frac{u}{2}\right)\left(\sin(u)\left(t\cdot\cos\left(\frac{u}{2}\right)+1\right)+\frac{t}{2}\sin\left(\frac{u}{2}\right)\cos(u)\right)\\&+\frac{t}{2}\cos^2\left(\frac{u}{2}\right)\cos(u)\end{aligned} \tag{104}$$

$$n_z = \cos\left(\frac{u}{2}\right)\left(t\cdot\cos\left(\frac{u}{2}\right)-1\right) \tag{105}$$

$$|\boldsymbol{n}| = \sqrt{1+\frac{t^2}{4}\left(3+2\cdot\cos(u)\right)+2t\cdot\cos\left(\frac{u}{2}\right)} \tag{106}$$

Equation (95) then becomes

$$Q(L) = \sigma\int_0^{2\pi}\int_{-l}^{l}\sqrt{1+\frac{t^2}{4}\left(3+2\cdot\cos(u)\right)+2t\cdot\cos\left(\frac{u}{2}\right)}\,\mathrm{d}t\mathrm{d}u \tag{107}$$

The inner integral could be exactly solved, followed by an appropriate numerical integration of the outer integral. Using linked terms

$$a_1 = 3+\cos(u) \tag{108}$$

$$b_1 = \frac{8}{L}\cdot\cos\left(\frac{u}{2}\right) \tag{109}$$

$$c_1 = \frac{L^2}{16}\left(\left(1+\frac{b_1}{a_1}\right)\sqrt{a_1+2b_1+\frac{16}{L^2}}+\left(1-\frac{b_1}{a_1}\right)\sqrt{a_1-2b_1+\frac{16}{L^2}}\right) \tag{110}$$

$$c_2 = \frac{a_1-4b_1}{a_1^{3/2}}\cdot\left(a_1+b_1+\ln\left(L\sqrt{a_1}\sqrt{a_1+2b_1+\frac{16}{L^2}}\right)\right) \tag{111}$$

$$c_3 = \frac{a_1-4b_1}{a_1^{3/2}}\cdot\left(-a_1+b_1-\ln\left(L\sqrt{a_1}\sqrt{a_1+2b_1+\frac{16}{L^2}}\right)\right) \tag{112}$$

we finally get for the outer integral

$$Q(L) = \sigma\int_0^{2\pi}\left(c_1+c_2+c_3\right)\mathrm{d}u \tag{113}$$

The calculation can be performed using a short *QBasic* program code given below. The numerical integration for $L = 1$ yields

$$Q(1) = 6.353271398\cdot\sigma = 2\pi\sigma\cdot 1.01115454786 \approx 2\pi\sigma\cdot\frac{12}{13}\sqrt{6/5} \tag{114}$$

with such an approximation we are faced again with *Fibonacci* number 13. Interestingly, the factor $\frac{r_c}{r_{sling}} = 1.011180106$ in Equation (62) approximates quite well the term 1.01115454786 within Equation (114). Combining both equations with the golden quartic polynomial result one finds again another numerical connection to the anomalous factor Δg_e as

$$\left(\frac{12}{13}\right)^{3/2}\cdot\frac{1}{\sqrt{5}\cdot 171} = 0.0023194\cdots \tag{115}$$

Consequences and the connection with the golden mean will be discussed in a following comprehensive contribution. Remarkable is also the approximate relation between number 13 and the circle constant π by solving the quadric equation

$$x^2+x-13 = 0 \tag{116}$$

giving

$$x_1 = 3.140054945 \tag{117}$$

when using the term 13.01119705 instead of the integer 13, the solution of the quadratic equation (116) delivers exactly the circle constant $\pi = 3.13159265\ldots$ With the aid of equation (114) one can decompose the term 13.01119705 into

$$13.01119705 \approx 12 + \frac{12}{13}\sqrt{\frac{6}{5}} = 12 + 1.011180106 \tag{118}$$

A.6. *QBasic* Program Code for Charge Calculation of a Moebius Strip (Width L = 1)

```
OPEN "O", #2, "moestrip.txt"
PI# = 3.14159265358979
BO# = PI# / 180
L = 1.1
SUM# = 0
FOR I = 1 TO 3600
    A# = COS(I * BO# / 10)
    B# = COS(I * BO# / 20)
    A1# = 2 * A# + 3
    B1# = 8 * B#/L
    TERM1# = (A1# + B1#) * SQR(A1# + 2 * B1# + 16/(L*L)) + (A1# - B1#) *
SQR(A1# - 2 * B1# + 16/(L*L)
    TERM2# = (A1# - 4*B#*B#) * (LOG(L*SQR(A1#) * SQR(A1# + 2 * B1# +
16/(L*L)) + A1# + B1#) - LOG(L*SQR(A1#) * SQR(A1# - 2 * B1# + 16/(L*L)) -
A1# +B1#))
    TERM1# = TERM1# * L * L /(16*A1#)
    TERM2# = TERM2# / (A1#)^(3/2)
    TERM# = TERM1# + TERM2#
    SUM# = SUM# + TERM#
NEXT I
SUM# = SUM# / 3600
SUM1# = SUM# *2 * PI#
PRINT #2, " Charge on a Moebius Stripe (L = 1)"
PRINT #2,
PRINT #2, USING " Q                ###.###############"; SUM1#
PRINT #2, USING " Q/(2*pi)    ###.###############"; SUM#
CLOSE #2
END
```

You may simply extend the code for arbitrary width L

Result:

Charge on a Moebius Stripe (L = 1)

Q	6.35327139844997
Q/(2*pi)	1.01115454786767